

## Spin glass behavior in rhombohedral $B_{12}$ cluster compounds

Takao Mori<sup>1,2,\*</sup> and Andreas Leithe-Jasper<sup>1,†</sup><sup>1</sup>National Institute for Materials Science, Advanced Materials Laboratory, Namiki 1-1, Tsukuba, 305-0044, Japan<sup>2</sup>PRESTO, Japan Science and Technology Agency (JST), Kawaguchi, 332-0012, Japan

(Received 23 September 2002; published 31 December 2002)

Magnetic properties of rhombohedral  $B_{12}$  cluster compounds  $RB_{22}C_2N$  ( $R=Er, Ho$ ) were investigated. The rare earth atoms are uniquely configured in corner-sharing deformed tetrahedra along the nearest-neighbor rare earth direction, with rare earth and  $B_6$  octahedral layers separated by  $B_{12}$  icosahedral and C-B-C chain layers. A drop in the zero-field-cooled magnetic susceptibility is observed at 5 K and 22.5 K for  $ErB_{22}C_2N$  and  $HoB_{22}C_2N$ , respectively. The magnetic susceptibility shows divergences for zero-field-cooled and field-cooled measurements, while the isothermal remanent magnetization decays as a stretched exponential of time  $\sigma_{IRM}(t) = \sigma_{I0} \exp[-C(\omega t)^{-(1-n)/(1-n)}]$ . Wait time effects on the thermal remanent magnetization are also observed. The measurements point to spin glass behavior in this system. The magnetic field dependence of the susceptibility peak temperature  $T_f$  is consistent with the well-known de Almeida–Thouless line, where  $H \propto [1 - T_f(H)/T_0]^{1.5}$ . The spin glass behavior is thought to be caused by disorder from partial occupancy of the rare earth atomic sites and also possible frustration of magnetic interactions. This is the first instance of a compound composed of rare earth atoms configured in a boron framework exhibiting glassiness and is also of interest in the context of recent new magnetism discovered in  $B_{12}$  icosahedral compounds. The low-temperature specific heat of  $ErB_{22}C_2N$  shows only a broad hump around the magnetic anomaly temperature and supports the absence of long-range order in this system.

DOI: 10.1103/PhysRevB.66.214419

PACS number(s): 75.50.Lk, 81.05.Je

### I. INTRODUCTION

The magnetic properties of frustrated systems exhibiting glassiness are a topic of longtime interest, and a search for such compounds has been actively carried out. Research has been done on a variety of compounds such as triangular lattice compounds,<sup>1</sup> kagomé compounds,<sup>2</sup> garnets,<sup>3,4</sup> olivines,<sup>5</sup> and the spin ice pyrochlores on which recent intriguing work has been done.<sup>6–8</sup> On the other hand, the magnetic properties of  $B_{12}$  icosahedral cluster compounds have also attracted interest following the discovery of an antiferromagnetic transition at relatively high temperatures in the magnetically dilute  $RB_{50}$  compounds which are nonmetallic.<sup>9–11</sup>

In this work, we report on the magnetic properties of the rhombohedral  $B_{12}$  cluster compounds  $ErB_{22}C_2N$  and  $HoB_{22}C_2N$ . Spin glass behavior is observed, with this system being the first higher boride compound where rare earth atoms reside in boron frameworks, in which such phenomena have been found.

### II. EXPERIMENT

The synthesis and structure determination of  $RB_{22}C_2N$  have been described previously.<sup>12</sup> The synthesis of the single-phase polycrystalline samples of  $ErB_{22}C_2N$  and  $HoB_{22}C_2N$  measured in this work was carried out in the following way. First of all, powders of  $RB_m$  ( $m:12–16$ ,  $R=Er, Ho$ ) were synthesized by the borothermal reduction of rare earth oxide under vacuum:



Then the desired amounts of boron, carbon, and hexagonal BN were added and fired again at a reaction temperature of

around 1700 °C. It is difficult to synthesize  $RB_{22}C_2N$  samples without impurity phases such as  $RB_6$  and  $RB_{12}$ . However, improved washing techniques of the sample were developed, such as boiling powdered samples for short times with nitric acid, and we found we could completely remove any traces of these impurity phases. The samples were characterized by using a high-resolution powder x-ray diffractometer (Rigaku Co., RINT2000) with Cu  $K\alpha$  radiation.  $RB_{22}C_2N$  is rhombohedral (space group  $R-3m$ ) with lattice constants of  $a=b=5.624 \text{ \AA}$ ,  $c=44.681 \text{ \AA}$  and  $a=b=5.614 \text{ \AA}$ ,  $c=44.625 \text{ \AA}$  for  $ErB_{22}C_2N$  and  $HoB_{22}C_2N$ , respectively. The structure is depicted in Figs. 1(a) and 1(b). The compound has a layered structure along the  $c$  axis with  $B_{12}$  icosahedral and C-B-C chain layers residing in between  $B_6$  octahedral and rare earth atomic layers. Figure 1(b) depicts the configuration of only the rare earth atoms and will be discussed later.

Magnetization was measured by using a Quantum Design superconducting quantum interference device (SQUID) magnetometer MPMS-XL from 1.8 K to 300 K and fields up to 5.5 T. For the time decay measurements of remanent magnetization, the starting point of time was determined by monitoring the voltage of the low-resolution current of the MPMS-XL magnet power supply and defining the effective zero field as when the voltage hovers at less than 1 mV, which is typically around 40–50 s earlier than the field stable message is displayed. Specific heat measurements were made on a piece cut off from a successfully sintered single-phase pellet of  $ErB_{22}C_2N$  using a transient heat pulse method with a small temperature increase of 2% relative to the system temperature.

### III. RESULTS AND DISCUSSION

The zero-field-cooled (ZFC) and field-cooled (FC) magnetic susceptibilities  $\chi$  of  $ErB_{22}C_2N$  are shown in Fig. 2(a).

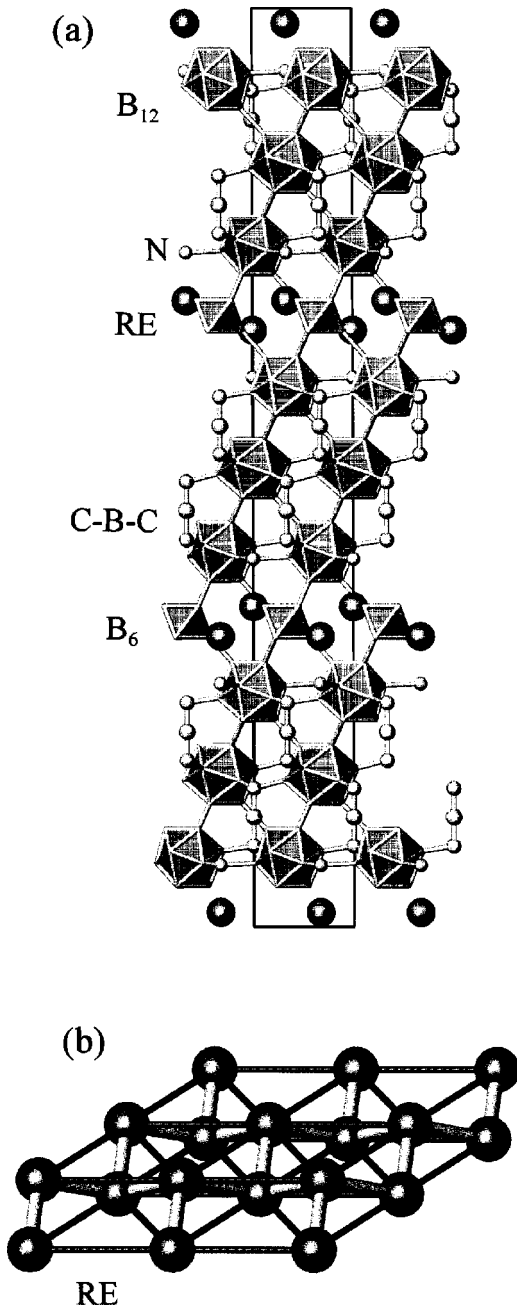


FIG. 1. Crystal structure of  $RB_{22}C_2N$ , (a) a view perpendicular to the  $c$  axis and (b) a view of the configuration of the rare earth atoms only. The large polyhedrons are  $B_{12}$  icosahedra, smaller polyhedrons indicate  $B_6$  octahedra, small circles indicate nitrogen atoms, the three bonded atoms along  $[0\ 0\ 1]$  are C-B-C chains, and the large circles indicate rare earth atoms.

A drop in the ZFC susceptibility is observed at around 5 K, indicating that some kind of transition has occurred. Strikingly, a large difference is observed for the ZFC and FC susceptibility curves, which indicates a magnetic ground state with high degeneracy. The temperature of the drop in susceptibility is similar to the antiferromagnetic transition temperature of  $ErB_{12}$  [ $T_N=6.6$  K (Ref. 13)], but due to our improved washing techniques used in preparation of the single-phase sample and, above of all, the fact that  $ErB_{12}$

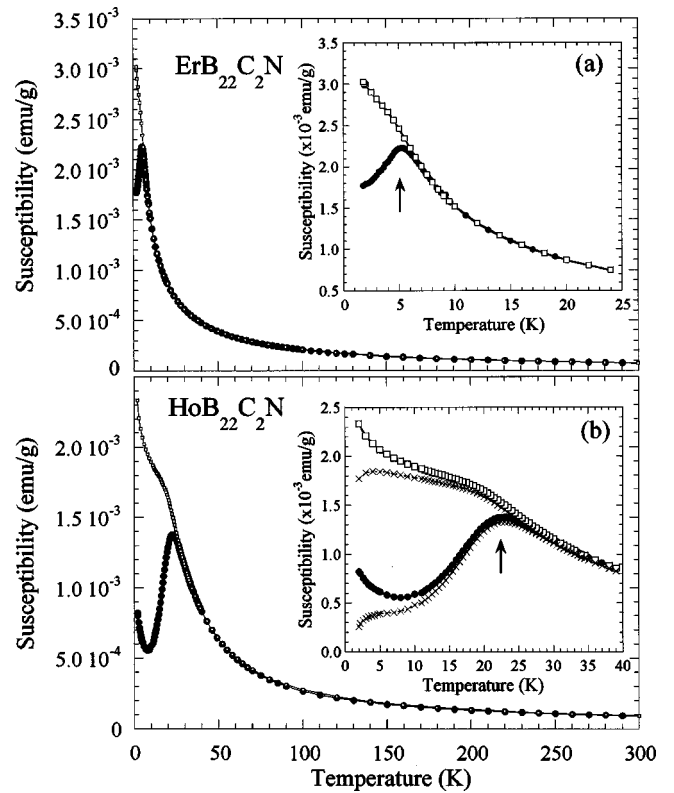


FIG. 2. Temperature dependence of the magnetic susceptibility of (a)  $ErB_{22}C_2N$  and (b)  $HoB_{22}C_2N$ . The insets are enlarged views of the low-temperature region. The magnetic field is 50 G. The crosses in the inset of (b) depict the susceptibility after the low-temperature Curie tail (see text) was subtracted. Arrows indicate the cusp temperature of the susceptibility  $T_f$ .

does not exhibit such a hysteresis in the magnetic susceptibility, we can conclude that this is an intrinsic property of  $ErB_{22}C_2N$ . The temperature of the peak which we label as  $T_f$  is determined from the derivative of the susceptibility (the temperature where  $d\chi/dT=0$ ) to be 5 K.

From the Curie-Weiss fitting

$$\chi = C/(T - \theta) \quad (2)$$

of the susceptibility curve at temperatures sufficiently above the magnetic anomaly ( $T \geq 40$  K), we obtain parameters of  $\theta = -7.0$  K and an effective magnetic moment  $\mu_{\text{eff}}$  of  $9.0\mu_B$  which is slightly smaller than the value of  $9.58\mu_B$  for a free trivalent Er ion.

$HoB_{22}C_2N$  shows similar behavior with the peak in the ZFC susceptibility occurring at  $T_f = 22.5$  K [Fig. 2(b)]. The high-temperature fit ( $T \geq 200$  K) yields  $\theta = -16.9$  K and  $\mu_{\text{eff}} = 10.1\mu_B$ .

It is of note that the FC susceptibility of  $RB_{22}C_2N$  shows a continued upturn at low temperatures below  $T_f$ . However, this behavior can be attributed to the existence of a low temperature Curie tail which is clearly apparent as the upturn in the ZFC curve of  $HoB_{22}C_2N$  [Fig. 2(b)]. The Curie tails are judged to not be an intrinsic feature of the magnetic anomaly observed in  $RB_{22}C_2N$  since they have also been observed for the  $RB_{50}$ -type compounds<sup>9-11</sup> and have been attributed to

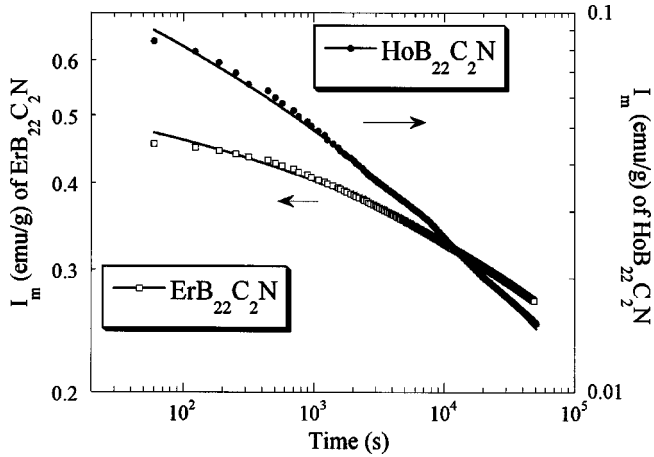


FIG. 3. Time evolution of the isothermal remanent magnetization  $\sigma_{\text{IRM}}$  of  $\text{ErB}_{22}\text{C}_2\text{N}$  at 2 K (solid circles) and  $\text{HoB}_{22}\text{C}_2\text{N}$  at 5 K (open squares). The lines depict the fit to  $\sigma_{\text{IRM}}(t) = \sigma_{\text{IRM}}(0)\exp[-C\omega t^{-(1-n)}]$ .

paramagnetic impurities such as  $\text{RB}_{66}$  or  $\text{RB}_{25}$  ( $R \neq \text{Tb}$ ), which are stable in acid, existing below the x-ray detection level, or to have some intrinsic origin the exact nature of which is not clear yet.<sup>11</sup> The magnitude of the low-temperature tail of  $\text{HoB}_{22}\text{C}_2\text{N}$ , for example, is approximately estimated by fitting the low-temperature region of the FC susceptibility as  $\chi = C/T + C_0$ .  $C = 1.1 \times 10^{-3}$  emu K/g, which is 4.0% of the Curie constant at high temperatures. The ZFC and FC susceptibility curves of  $\text{HoB}_{22}\text{C}_2\text{N}$  after the Curie component was subtracted are shown in the inset of Fig. 2(b). The slight downturn of the curves at the lowest temperatures might indicate that there is also a small Curie-Weiss component with low Weiss temperature (such as  $\text{HoB}_{25}$ ,  $\text{HoB}_{66}$ ) of which the contribution at low temperatures was overestimated by assuming only a  $C/T$  form. In any case, it appears that the pronounced upturn of the  $\chi$  curves can be generally explained by such a Curie tail. We did not attempt this procedure for  $\text{ErB}_{22}\text{C}_2\text{N}$  as the temperature of the magnetic anomaly is low.

The specific heat measurements discussed later exclude a low-magnetic-field-induced transition from an antiferromagnetic state to a partly paramagnetic or ferromagnetic state, for example, as a possible explanation of the divergence of the ZFC and FC susceptibility curves.

Strikingly, the isothermal remanent magnetization  $\sigma_{\text{IRM}}$  of  $\text{RB}_{22}\text{C}_2\text{N}$  at low temperatures shows a gradual decay over several decades of time. The time evolution of  $\sigma_{\text{IRM}}$  is plotted in Fig. 3. The samples were cooled to 2 K and 5 K for  $\text{ErB}_{22}\text{C}_2\text{N}$  and  $\text{HoB}_{22}\text{C}_2\text{N}$ , respectively. A field of 10 kG was applied for 5 min after which the field was charged to zero and  $\sigma_{\text{IRM}}$  measured. The time dependence can be described by a stretched exponential

$$\sigma_{\text{IRM}}(t) = \sigma_{\text{I0}} \exp[-C\omega t^{-(1-n)/(1-n)}], \quad (3)$$

the dependence of which has been typically observed for some spin glasses.<sup>14,15</sup>  $\sigma_{\text{I0}} = 0.61$  emu/g,  $C\omega^{-(1-n)/(1-n)} = 0.12$  s<sup>1/(1-n)</sup>,  $1-n = 0.18$  and  $\sigma_{\text{I0}} = 0.53$  emu/g,  $C\omega^{-(1-n)/(1-n)} = 1.2$  s<sup>1/(1-n)</sup>,  $1-n = 0.10$  for  $\text{ErB}_{22}\text{C}_2\text{N}$

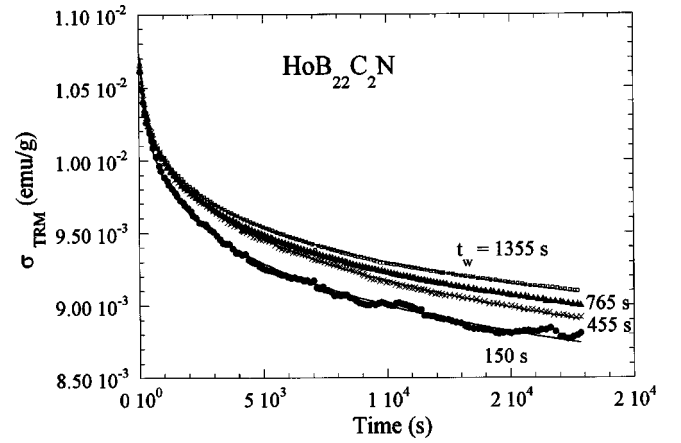


FIG. 4. Time evolution of the thermal remanent magnetization  $\sigma_{\text{TRM}}$  of  $\text{HoB}_{22}\text{C}_2\text{N}$  at 10 K for different wait times of  $t_w$  of 150 s (solid circles), 455 s (crosses), 765 s (solid triangles), and 1355 s (open squares). The measurements were carried out by 10 G field cooling from 30 K to 10 K, with  $t_w$  defined as the time from when the sample passes through  $T_f = 22.5$  K until the field is charged to 0 G at 10 K. The lines depict the stretched exponential fits.

and  $\text{HoB}_{22}\text{C}_2\text{N}$ , respectively. The reduced temperature  $T_r = T/T_f$  is 0.40 and 0.22 while  $1-n$  take values of 0.18 and 0.10 for the Er and Ho phases, respectively. The relative magnitudes agree with the empirical  $T_r$  dependence of  $1-n$  determined by Hoogerbeets *et al.* for some typical spin glass systems.<sup>16</sup> As a physical picture, the stretched exponential relaxation in spin glasses has been explained by various models such as the fractal cluster model of Continentino and Malozemoff,<sup>17</sup> although absolute values of experimentally determined parameters have not always been satisfactorily explained.

The divergence of the ZFC and FC susceptibility curves (we note that the low-temperature upturn in the FC susceptibility can generally be attributed to a low-temperature Curie tail) and the gradual relaxation of the isothermal remanent magnetization over several decades of time is indicative of spin glass behavior.<sup>14</sup>

Wait time effects are a distinctive signature of spin glass systems. To further investigate the magnetic behavior of this system, wait time effects on the thermal remanent magnetization  $\sigma_{\text{TRM}}$  of  $\text{HoB}_{22}\text{C}_2\text{N}$  were investigated.  $\sigma_{\text{TRM}}$  was measured by applying a low magnetic field of 10 G at 30 K and then field cooling down below  $T_f$  to 10 K. After waiting for variable times the field is charged to 0 G. The wait time  $t_w$  is calculated as the time since the sample passes through  $T_f = 22.5$  K until the field is switched to zero.  $\sigma_{\text{TRM}}$  for  $t_w = 150$  s, 455 s, 765 s, and 1355 s are plotted in Fig. 4. As can be seen, wait time effects are indeed observed, with the decay of  $\sigma_{\text{TRM}}$  appearing to be more gradual for longer  $t_w$ . Fits to Eq. (3) yielded parameters which are analyzed as follows.  $1-n$  versus the logarithmic of  $C\omega^{-(1-n)}$  is plotted in Fig. 5(a). A straight line extrapolation of the plot yields  $C = 0.033$ .  $\omega$  can then be determined and  $\log \omega$  is plotted in Fig. 5(b) versus  $t_w$ . The data approximately follow a straight line and can be fitted satisfactorily by

$$\omega = \omega_0 \exp[-t_w/t_0], \quad (4)$$

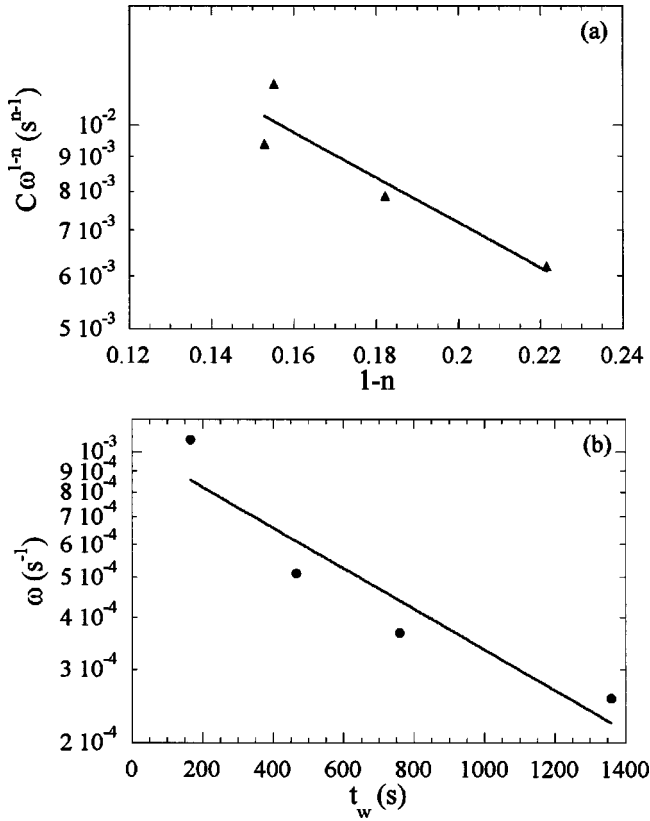


FIG. 5. The (a) logarithmic of  $C\omega^{-(1-n)}$  as a function of  $1-n$  determined from the measurements plotted in Fig. 4 and the (b) logarithmic of  $\omega$  plotted vs the wait time  $t_w$ . The lines depict the respective fits to exponentials.

where  $\omega_0 = 1.0 \times 10^{-3} \text{ s}^{-1}$  and  $t_0 = 8.9 \times 10^2 \text{ s}$ . This behavior is similar to the wait time effects first described by Chamberlin for a typical spin glass.<sup>18</sup>

The magnetization curves of  $\text{RB}_{22}\text{C}_2\text{N}$  measured at these temperatures showed hysteresis as expected from the remanent magnetization measurements, and a lack of saturation indicated the absence of long-range order in this system which is also consistent with a spin glass compound.

The magnetic field dependence of the magnetic susceptibility was also investigated. The susceptibility curves at several varying fields are shown in Fig. 6.  $T_f$  shifts to lower temperature at higher fields. It can also be clearly observed by comparing the 50 G and 5 kG curves that the peak structure of the susceptibility broadens at the higher field. As was seen in Fig. 2, there appears to be a wide weak irreversibility region above  $T_f$ . It was not easy to objectively define thresholds and definitely determine border temperatures for the onset of weak and also strong irreversibility. Therefore, we consider  $T_f$  as a measure of the onset of strong irreversibility in our system and plot the magnetic field dependence of  $T_f(H)$  in Fig. 7. It has been observed in many spin glasses that the boundary of strong irreversibility can be well described by the de Almeida–Thouless (AT) line.<sup>19</sup> The best fit of our data to the equation

$$H = H_0[1 - T_f(H)/T_0]^{1.5}, \quad (5)$$

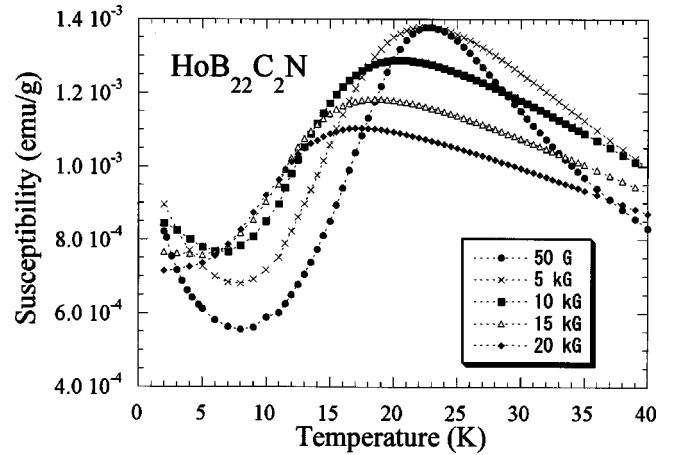


FIG. 6. Temperature dependence of the zero-field-cooled susceptibility of  $\text{HoB}_{22}\text{C}_2\text{N}$  for varying magnetic fields 50 G (solid circles), 5 kG (crosses), 10 kG (solid squares), 15 kG (open triangles), and 20 kG (open diamonds). The data for the 50 G curve are the same as that shown in Fig. 2(b).

where  $H_0 = 1.8 \times 10^5 \text{ G}$  and  $T_0 = 23 \text{ K}$ , is shown by the line in Fig. 7 and found to not be a bad representation.

The measurements discussed above are all indicative of spin glass behavior. It has generally been pointed out that in addition to disorder some frustration of the magnetic interactions are typically necessary ingredients of spin glass states.<sup>14</sup> In some systems such as the pyrochlore  $\text{Tb}_2\text{Mo}_2\text{O}_7$  which have strong magnetic frustration that is geometric in origin, it has been demonstrated that even with the absence of disorder, the manifestation of a spin glass state is possible.<sup>20</sup> However, in our system the frustration indexes  $f_{\text{frus}} = |\theta|/T_f = 0.75$  for  $\text{HoB}_{22}\text{C}_2\text{N}$  and  $f_{\text{frus}} = 1.4$  for  $\text{ErB}_{22}\text{C}_2\text{N}$  are not very large and so, therefore, such a strong frustration as would solely cause a spin glass state is not indicated. In  $\text{RB}_{22}\text{C}_2\text{N}$ , the partial occupancy of 0.74 of the rare earth atomic sites can be considered to be a source for disorder. We have previously observed a long-range-order AF transition for another rare earth  $\text{B}_{12}$  cluster compound  $\text{GdB}_{18}\text{Si}_5$ .<sup>21</sup> The rare earth atomic sites of  $\text{GdB}_{18}\text{Si}_5$  are also

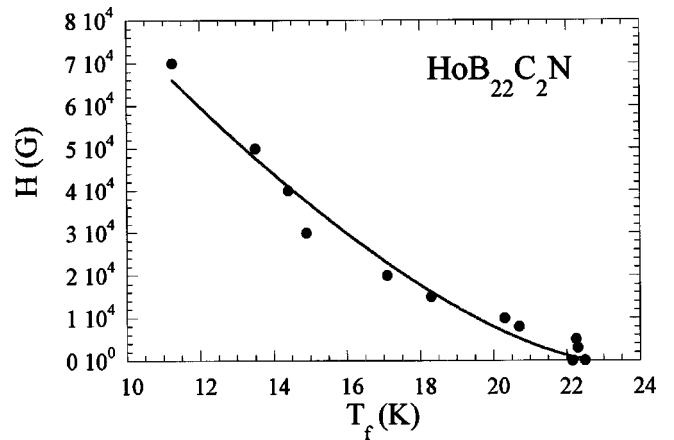


FIG. 7. Magnetic field dependence of  $T_f$  for  $\text{HoB}_{22}\text{C}_2\text{N}$ . The line describes the best fit of the data to Eq. (5).

partially occupied with an even lower occupancy of 0.68, so of course although the systems have different structures, we are inclined to think that such disorder by itself is solely not sufficient to cause the spin glass behavior in this system and that it is likely that there is also some frustration of magnetic interactions in  $RB_{22}C_2N$ .

We examine the configuration of the rare earth atoms in this compound which has been depicted in Fig. 1(b) and is unique. The rare earth atomic layers are separated by approximately 15 Å along the  $c$  axis, and therefore it is indicated that any sizable magnetic interaction will be among rare earth atoms within the layers. Within the layers the rare earth atoms form two regular triangular layers closely laid on top of one another. In the nearest-neighbor rare earth direction [indicated by the thick bonds in Fig. 1(b), with a separation of 3.54 Å] a rare earth atom in one layer is connected to three rare earth atoms in the adjacent layer, forming corner-sharing deformed tetrahedra. The separation of the rare earth atoms in the regular triangular layer which is parallel to the basal  $a$ - $b$  plane [indicated by the thin bonds in Fig. 1(b)] is 5.62 Å.

The high-temperature susceptibility data with negative Curie-Weiss temperature  $\theta$  indicate an antiferromagnetic AF interaction. In our system, if an AF interaction along the nearest-neighbor direction (thick bonds), which we label as  $J_0$ , were dominant, then there would be no frustration, since a minimization of energy would be satisfied with a configuration where the spins are ferromagnetically aligned within the triangular layers and the layers themselves are antiferromagnetically ordered. However, since it is likely that some degree of magnetic frustration exists, it is indicated that the interaction within the triangular layers (thin bonds), which we label as  $J_1$ , is antiferromagnetic and of comparable magnitude or larger than  $J_0$ .

The explicit mechanism of the magnetic interaction in this system is not clear at present. The Curie-Weiss temperature  $\theta$  determined at high temperatures should be an indication of the magnitude of the antiferromagnetic interaction between the rare earth atoms.  $\theta$  is  $-7.0$  K and  $-16.9$  K for  $ErB_{22}C_2N$  and  $HoB_{22}C_2N$ , respectively. The relative magnitude of  $\theta$  does not match either the de Gennes factor dependence of a simple RKKY-mediated interaction<sup>22</sup> or that of a dipole-dipole interaction which would approximately be proportional to  $g_J^2 \mu_B^2 J(J+1)$  (where  $g_J$  is the Lande factor and  $J$  the total angular momentum). It has previously been indicated for some B<sub>12</sub> icosahedral compounds such as  $RB_{50}$ , that a sizable magnetic interaction is mediated by the B<sub>12</sub> icosahedra.<sup>9-11,21,23</sup> From the structure of  $RB_{22}C_2N$ , such an interaction could be effective between the rare earth atoms within the triangular layers adjacent to the B<sub>12</sub> clusters and be the origin of  $J_1$ . The B<sub>6</sub> octahedra situated among the rare earth layers could be playing a role in mediating the magnetic interaction  $J_0$ . Theoretical work is presently being done on solving the explicit mechanism in such systems. In any case, the likely existence of magnetic frustration in  $RB_{22}C_2N$  indicates that despite the considerably shorter rare earth separation, the interaction of rare earth atoms between

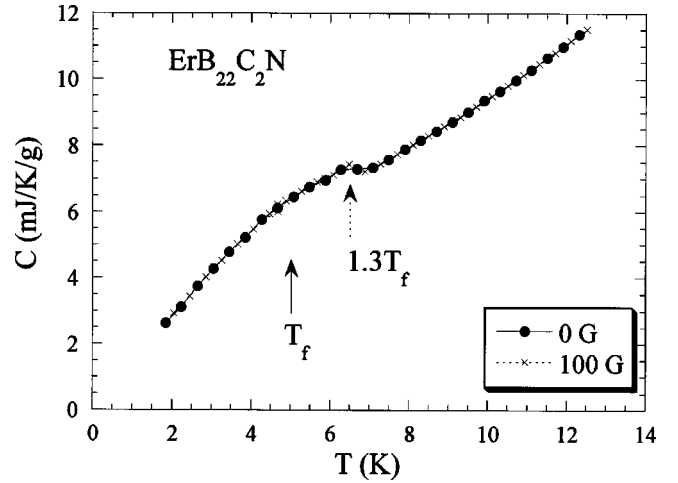


FIG. 8. Temperature dependence of the low-temperature specific heat of  $ErB_{22}C_2N$  under 0 G (solid circles) and under a magnetic field of 100 G (crosses). The solid arrow indicates the temperature of the cusp in the ZFC magnetic susceptibility  $T_f=5$  K, while the dotted arrow indicates  $1.3T_f$ .

adjacent triangular layers  $J_0$  is comparable or smaller than the interaction within the basal plane rare earth triangular layers  $J_1$ .

The specific heat of  $ErB_{22}C_2N$  at low temperatures was measured and is shown in Fig. 8. Only a broad hump in the specific heat is observed around the temperature of the cusp in the zero-field-cooled magnetic susceptibility  $T_f=5$  K with a peak at a higher temperatures around  $1.3T_f$ . This behavior is consistent with a spin glass state<sup>14</sup> and points to the absence of long-range ordering of the magnetic moments. The specific heat of  $ErB_{22}C_2N$  measured under a magnetic field of 100 G is also plotted. No sizable difference is observed between the specific heat measured at 0 G and at 100 G. This excludes the possibility of a low-field-induced transition from an antiferromagnetic state to a partly paramagnetic or ferromagnetic state to alternately possibly explain the low-temperature behavior of the 50 G ZFC and FC susceptibilities observed in Fig. 2 which we have mainly attributed to a Curie tail.

#### IV. CONCLUSIONS

The magnetism of rhombohedral B<sub>12</sub> cluster compounds  $ErB_{22}C_2N$  and  $HoB_{22}C_2N$  was investigated. The compounds have a layered structure along the  $c$  axis with B<sub>12</sub> icosahedral and C-B-C chain layers residing in between B<sub>6</sub> octahedral and rare earth atomic layers. A drop in the zero-field-cooled magnetic susceptibility is observed around 5 K and 22 K for  $ErB_{22}C_2N$  and  $HoB_{22}C_2N$ , respectively. (1) Divergences of the ZFC and FC susceptibility curves, (2) relaxation of the isothermal remanent magnetization, and (3) existence of wait time effects were observed, which are all indicative of spin glass behavior. The spin glass behavior in this system is thought to be caused by disorder from partial occupancy of the rare earth atomic sites and also likely frustration of magnetic interactions. Frustration would indicate that the magnetic interaction between the rare earth atoms along the short

bonds of the corner-sharing deformed tetrahedra is comparable or smaller than the interaction within the basal plane rare earth triangular layers. This is the first report of rare earth atoms configured in a boron framework exhibiting glassiness. New developments based on this work can be expected, since the framework accommodating the rare earth atoms in boron cluster compounds has been known to take a myriad variety of structures, and modifications are also possible with additional doping of such elements as silicon and carbon. This finding is also interesting in the context of the

ongoing investigation into boron clusters as new agents of mediating magnetic interaction.

#### ACKNOWLEDGMENTS

The authors are greatly indebted to E. Takayama-Muromachi for discussions and help with the measurements. F. Zhang is also thanked for assistance. This work was partially supported by Special Coordination Funds.

\*Corresponding author. Email address: mori.takao@nims.go.jp

<sup>†</sup>Present address: Max Planck-Institut für Chemische Physik fester Stoffe, Nothnitzer Str. 40, 01187 Dresden, Germany.

<sup>1</sup>H. Serrano-Gonzalez, S. T. Bramwell, K. D. M. Harris, B. M. Kariuki, L. Nixon, I. P. Parkin, and C. Ritter, *Phys. Rev. B* **59**, 14 451 (1999) and references therein.

<sup>2</sup>C. Broholm, G. Aeppli, G. P. Espinosa, and A. S. Cooper, *Phys. Rev. Lett.* **65**, 3173 (1990).

<sup>3</sup>P. Schiffer, A. P. Ramirez, D. A. Huse, and A. J. Valentino, *Phys. Rev. Lett.* **73**, 2500 (1994).

<sup>4</sup>S. R. Dunsiger *et al.*, *Phys. Rev. Lett.* **85**, 3504 (2000).

<sup>5</sup>I. S. Hagemann, P. G. Khalifah, A. P. Ramirez, and R. J. Cava, *Phys. Rev. B* **62**, R771 (2000).

<sup>6</sup>M. J. Harris, S. T. Bramwell, D. F. McMorrow, T. Zeiske, and K. W. Godfrey, *Phys. Rev. Lett.* **79**, 2554 (1997).

<sup>7</sup>A. P. Ramirez, A. Hayashi, R. J. Cava, R. Siddharthan, and B. S. Shastry, *Nature (London)* **399**, 333 (1999).

<sup>8</sup>S. T. Bramwell *et al.*, *Phys. Rev. Lett.* **87**, 047205 (2001).

<sup>9</sup>T. Mori and T. Tanaka, *J. Phys. Soc. Jpn.* **68**, 2033 (1999).

<sup>10</sup>T. Mori and T. Tanaka, *J. Phys. Soc. Jpn.* **69**, 579 (2000).

<sup>11</sup>T. Mori and T. Tanaka, *IEEE Trans. Magn.* **37**, 2144 (2001).

<sup>12</sup>F.X. Zhang, F.F. Xu, A. Leithe-Jasper, T. Mori, T. Tanaka, A.

Sato, P. Salamakha, and Y. Bando, *J. Solid State Chem.* **159**, 174 (2001).

<sup>13</sup>H. Misiorek, J. Mucha, A. Jezowski, Y. Paderno, and N. Shitsevalova, *J. Phys.: Condens. Matter* **7**, 8927 (1995).

<sup>14</sup>K. Binder and A. P. Young, *Rev. Mod. Phys.* **58**, 801 (1986).

<sup>15</sup>R. V. Chamberlin, G. Mozurkewich, and R. Orbach, *Phys. Rev. Lett.* **52**, 867 (1984).

<sup>16</sup>R. Hoogerbeets, W. L. Luo, and R. Orbach, *Phys. Rev. B* **34**, 1719 (1986).

<sup>17</sup>M. A. Continentino and A. P. Malozemoff, *Phys. Rev. B* **33**, 3591 (1986).

<sup>18</sup>R. V. Chamberlin, *Phys. Rev. B* **30**, 5393 (1984).

<sup>19</sup>J. R. L. De Almeida and D. J. Thouless, *J. Phys. A* **11**, 983 (1978).

<sup>20</sup>B. D. Gaulin, J. N. Reimers, T. E. Mason, J. E. Greedan, and Z. Tun, *Phys. Rev. Lett.* **69**, 3244 (1992).

<sup>21</sup>T. Mori and F. Zhang, *J. Phys.: Condens. Matter* **14**, 11831 (2002).

<sup>22</sup>M. A. Ruderman and C. Kittel, *Phys. Rev.* **96**, 99 (1954); T. Kasuya, *Prog. Theor. Phys.* **16**, 45 (1956); K. Yoshida, *Phys. Rev.* **106**, 893 (1957).

<sup>23</sup>T. Mori, F. Zhang, and T. Tanaka, *J. Phys.: Condens. Matter* **13**, L423 (2001).